Chinese Journal of
POLYMER SCIENCE

RESEARCH ARTICLE

https://doi.org/10.1007/s10118-026-3798-z
Chinese J. Polym. Sci.

The Effect of Curing Cycle on Interlaminar Shear Strength and Thermal Properties of Carbon Fiber Composite of High Temperature Maleimide-containing Phthalonitrile Dual-curing Resin

Hassan Fattahi*, Milad Hatami, Mohammad Reza Ehsani, and Mehrzad Mortezaei

Department of Polymer Engineering, Composite Research Institute, Faculty of Materials and Manufacturing Technologies, Malek Ashtar University of Technology, Tehran 1774-15875, Iran

Abstract In this study, a phthalonitrile monomer containing a maleimide group (MPN) with a melting point of 106.8 °C was successfully synthesized. Differential scanning calorimetry (DSC) showed that the MPN resin can act as an autocatalyzed resin without any curing agent. The monomer was then cured using diallyl bisphenol A (DABA) as the curing agent. Based on the results of FTIR analysis, a suitable curing cycle was established. Given the dual-stage curing behavior of the monomer, three composite samples were fabricated using three different curing cycles to investigate the relationship between the polymer structure and final properties. Interlaminar shear strength (ILSS) tests showed that samples with approximately 95% curing degree for the phthalonitrile part of this resin exhibited an ILSS of approximately 37.5 MPa. Dynamic mechanical thermal analysis (DMTA) confirmed the formation of a thermally stable and rigid crosslinked network in the synthesized composite. The storage modulus (E') exhibited relatively high values even at incomplete curing stages, maintaining significant stiffness up to approximately 100 °C, which highlights the early formation of a semi-crosslinked structure. Thermogravimetric analysis (TGA) revealed that the fabricated composite had good thermal resistance with $T_{5\%}$ and $T_{10\%}$ of 484 and 584 °C, respectively, with a char yield of 84% at 900 °C.

Keywords High temperature resin; Phthalonitrile; Maleimide; Dual-curing resin; Interlaminar shear strength

Citation: Fattahi, H.; Hatami, M.; Ehsani, M. R.; Mortezaei, M. The effect of curing cycle on interlaminar shear strength and thermal properties of carbon fiber composite of high temperature maleimide-containing phthalonitrile dual-curing resin. *Chinese J. Polym. Sci.* https://doi.org/10.1007/s10118-026-3798-z

INTRODUCTION

High-performance resins have attracted significant attention in recent decades owing to their critical role in advanced technologies that require materials with superior thermal and mechanical properties. Their combination of high thermal stability, outstanding mechanical strength, and excellent processing performance makes them indispensable in sectors such as aerospace, defense, electronics, energy, and advanced composites.[1–3] In these areas, where the operational conditions often involve extreme temperatures, mechanical stresses, and chemically aggressive environments, the choice of structural materials can determine the safety, durability, and cost-effectiveness of the system.

Within the broad category of thermosetting polymers, many classes of heat-resistant resins have been developed and commercialized, each with distinct advantages and limitations. Benzoxazines,[4–6] epoxies,[7–9] propargylated and allylated phenolics,[10–15] cyanate esters,[16–19] bismaleimides,[20–23] and phthalonitriles[24–27] represent prominent examples of such systems. These resins share common features such as high glass-transition temperatures, chemical resistance, and stable crosslinked networks. However, differences in their molecular structures dictate their performance envelopes and processabilities. Among them, phthalonitrile (PN) resins stand out due to their unique ability to form heteroaromatic triazine and phthalocyanine ring structures during polymerization, imparting remarkable flame retardancy, outstanding thermal resistance, and superior mechanical integrity.[28,29] These features have positioned PN resins as promising candidates for use in aerospace, shipbuilding, marine engineering, and microelectronics, where both high reliability and long service lifetimes are required.[30,31]

However, despite these advantages, the industrial application of PN resins faces significant challenges. The most important of these is their poor processability, which is a consequence of the inherent inertness of the nitrile group. Polymerization typically requires extremely high curing temperatures and prolonged processing cycles, which not only limits efficiency, but also increases costs and restricts compatibility with other matrix materials.[32] Considerable research efforts have been directed towards overcoming these shortcomings. One approach involves the use of curing accelerators such as

* Corresponding author, E-mail: fattahi@mut.ac.ir, hassan.fattahi@gmail.com
Received May 17, 2026; Accepted June 30, 2026; Published online August 28, 2026

metal salts,[33] phenolic compounds,[34] aromatic amines,[35] and strong organic acids,[35] which can lower the activation energy for curing and reduce cycle times.

Another strategy is molecular modification, where flexible linkages, such as aryl[36] or alkyl ethers,[37] are introduced to reduce melting points and enhance processability. While effective, these modifications can negatively impact thermal stability, diminishing one of PN's most valuable attributes of PN. Recent advances have focused on incorporating reactive functional groups, such as amino or hydroxyl moieties, directly into PN monomers. These groups promote autocatalytic curing and enable the formation of highly crosslinked networks without additional curing agents, representing a promising path for balancing processability and performance.[38]

Along with these developments, maleimide-based resins have emerged as an important class of high-performance thermosets. Bismaleimide (BMI) resins, in particular, are widely recognized for their excellent thermal resistance, mechanical strength, low coefficients of thermal expansion, and inherent flame retardancy.[39–43] These features have driven their applications in aerospace, advanced electronics, and renewable energy technologies. However, their high crosslink density leads to brittleness and reduced toughness, and limits their use in applications involving dynamic loading or impact.[20] To overcome this shortcoming, numerous modification strategies have been investigated, including the introduction of flexible ether linkages into BMI monomers, use of diamine chain extenders to increase segmental mobility, and copolymerization with allyl compounds to improve toughness. These approaches highlight the importance of structural design for balancing the mechanical robustness and processability of maleimide systems.

Recent research has explored the synergistic integration of BMI units into PN molecular structures. This hybridization aims to combine the outstanding thermal and mechanical properties of PN with the enhanced processability and reactivity of the BMI. Studies have demonstrated that BMI-modified PN resins can exhibit improved curing efficiency, higher crosslink densities, and superior moisture resistance, expanding their potential for high-performance applications.[44–46]

For instance, Kaliavaradhan *et al.*[47] synthesized BMI-containing PN systems using different phenylene diamine isomers and demonstrated excellent thermal stability and moisture resistance. Similarly, Nechausov *et al.*[48] reported the development of maleimide-capped PN compounds *via* the reaction of aminophenoxy PN with maleic anhydride. However, the resulting para- and ortho-isomers exhibited relatively high melting points (210 and 200 °C, respectively), necessitating further structural optimization and the use of comonomers to improve their processability. These findings highlight both the promise and limitations of current approaches, emphasizing the need for new molecular designs that can lower melting points without compromising performance.

In this context, the present study addresses this critical gap by focusing on the design and synthesis of a phthalonitrile resin containing a maleimide group with a low melting point. This design strategy is intended to expand the processing window of PN resins, thereby enhancing their processability in industrial applications. To evaluate the performance of the synthesized resin, the monomer was cured with diallyl bisphenol A (DABA), and the resulting materials were systematically investigated for their thermal stability, curing behavior, and mechanical properties. By combining the favorable attributes of PN and BMI chemistries, this study seeks to provide new insights into the development of next-generation high-performance resins for aerospace, electronics, and other demanding applications.

EXPERIMENTAL

Materials

4-Nitrophthalonitrile (NPN), 3-aminophenol, potassium carbonate (K_2CO_3), magnesium sulfate ($MgSO_4$), dimethylformamide (DMF), sodium hydroxide (NaOH), maleic anhydride, acetone, sodium sulfate (Na_2SO_4), acetic anhydride, sodium acetate, and diallyl bisphenol A (DABA) were purchased from Merck and used without further purification. Carbon fibers with an areal weight of 200 g/m^2 were used as the reinforcement material for the preparation of the composite.

Synthesis of 4-(3-Aminophenoxy) Phthalonitrile (APPN)

In a two-necked round-bottom flask, 3.78 g (0.035 mol) of 3-aminophenol, 6 g (0.035 mol), and DMF (25 mL) were added to a two-necked round-bottom flask. The mixture was magnetically stirred until a homogeneous solution was obtained. Then, 7.81 g (0.052 mol) of potassium carbonate was added to the reaction mixture. The reaction was carried out under a nitrogen atmosphere at 85 °C for 5 h. After cooling to room temperature, the resulting brown product was poured into 0.1 mol/L sodium hydroxide solution. The solid was separated, washed with distilled water until neutralized, and dried in a vacuum oven at 80 °C. A brown powder was obtained in a 90% yield.

Synthesis of the 4-(3-Maleimidophenoxy)phthalonitrile Monomer (MPN)

A total of 2.93 g (0.03 mol) of maleic anhydride was dissolved in 40 mL of dry acetone and transferred to a 250 mL two-necked round-bottom flask. Then, 6.42 g (0.027 mol) of APPN was dissolved in 50 mL of dry acetone and added dropwise to the maleic anhydride solution under magnetic stirring over 30 min using a dropping funnel. The temperature of the oil bath was then increased to 60 °C and the reaction mixture was refluxed under a nitrogen atmosphere for 1 h. At this stage, a brown intermediate insoluble in acetone, referred to as amic acid, was formed.

Subsequently, 3.37 mL (0.036 mol) of acetic anhydride and 0.22 g (0.003 mol) of sodium acetate were added to the reaction mixture. The mixture was refluxed for 4 h under the same conditions as in the previous step. After the completion of the reaction, the resulting brown solid was precipitated by a solvent/non-solvent method using ice-cold water. Finally, the supernatant was decanted, and the obtained solid was washed several times with distilled water, followed by several washes with 10 wt% aqueous sodium carbonate solution, and then dried in an oven at 50 °C.

Curing of MPN Resin with Diallyl Bisphenol A

To curing of the monomer, 4 g of the MPN monomer was heat-

ed at 120 °C under magnetic stirring for 10 min until fully melted. Then, diallyl bisphenol A (DABA) was added at 21 wt% relative to the resin, and stirring was continued for an additional 5 min to obtain a homogeneous solution with the appropriate viscosity. The curing cycles are listed in Table 1.

Table 1 Curing cycles codes applied for curing of MPN resin.

Symbol	Curing cycle
(a)	Before curing
(b)	30 min @ 200 °C
(c)	1 h @ 200 °C
(d)	2 h @ 200 °C
(e)	2 h @ 200 °C + 4 h @ 315 °C
(f)	2 h @ 200 °C + 6 h @ 315 °C
(g)	2 h @ 200 °C + 8 h @ 315 °C
(h)	2 h @ 200 °C + 10 h @ 315 °C
(i)	2 h @ 200 °C + 10 h @ 315 °C + 2 h @ 350 °C
(j)	2 h @ 200 °C + 10 h @ 315 °C + 6 h @ 350 °C

Preparation of Carbon/Phthalonitrile Composite

A carbon fiber mat with a density of 1.78 g/cm^3 and nominal thickness of 0.25 mm was used as the reinforcement material. Composite laminates were fabricated using a hand-lay-up process. During fabrication, the carbon fiber mats were impregnated with the MPN/DABA resin system and stacked layer by layer to obtain the desired laminate structure. To fabricate a 10-layer carbon/MPN composite, 1.26 g of resin was required. However, considering the resin loss during the hand lay-up process, 4 g of the resin was used for impregnation. The Impregnation was carried out by the melt method on a hot plate at a resin's melting temperature, approximately 120 °C. After complete impregnation of the carbon fibers with the MPN resin, the prepreg fabric was allowed to cool to room temperature to solidify the resin. The fabric was then cut into ten equal pieces with dimensions of 5 cm × 4 cm. The lay-up process was performed at 150 °C to ensure interlayer resin flow and bonding, and the sample was then placed in a mold and prepared for curing.

Characterization

FTIR analysis

FTIR analysis was performed using a Thermo Fisher Scientific (USA) spectrometer in the range 4000–400 cm^{-1}. This technique was employed for both identification and structural analysis during monomer synthesis, and for monitoring the curing behavior of the synthesized resin. The degree of curing (DOC) was calculated from the area under the peak, using Eq. (1):

$$\mathrm{DOC} = \left(\frac{(A_{\mathrm{reactivebond}})_0 - (A_{\mathrm{reactivebond}})_t}{(A_{\mathrm{reactivebond}})_0}\right. \quad (1)$$

In Eq. (1), $(A_{\mathrm{reactivebond}})_t$ and $(A_{\mathrm{reactivebond}})_0$ are the areas under the peaks at 700 and 2223 cm^{-1}, which are the main characteristic peaks of the maleimide and cyanide groups at time t and $t = 0$, respectively.

Elemental analysis

Elemental analysis (CHN) was performed using a Perkin-Elmer 2400 II instrument (USA) to confirm the elemental composition of the MPN monomer.

NMR analysis

Proton nuclear magnetic resonance (^{1}H-NMR) analysis was performed using a Bruker Ultra Shield 400 MHz spectrometer (Bruker, Germany). To further evaluate the synthesized MPN monomer, carbon nuclear magnetic resonance (^{13}C-NMR) analysis was performed using a 400 MHz Bruker UltraShield spectrometer (Bruker, Germany). The synthesized resin was characterized using deuterated dimethyl sulfoxide (DMSO-d_6) as solvent.

Differential scanning calorimetry (DSC)

DSC analysis was conducted using a NETZSCH 200 F3 instrument (Germany) to investigate the curing behavior of the MPN resin. The analysis was performed from room temperature to 350 °C, at a heating rate of 10 °C/min.

Thermogravimetric analysis (TGA)

TGA was performed using a Mettler-Toledo (Switzerland) instrument to evaluate the thermal stability and weight loss behavior of the carbon fiber/phthalonitrile composite. The test was performed from room temperature up to 900 °C at a heating rate of 10 °C/min under an argon atmosphere.

Interlaminar shear strength (ILSS)

ILSS of the MPN/carbon fiber composite was measured using an ILSS testing machine at a crosshead speed of 2 mm/min according to ASTM D-2344.[49]

Dynamic mechanical thermal analysis (DMTA)

To investigate the dynamic mechanical thermal properties of the cured MPN resin and the carbon fiber/MPN composite, a DMTA device (model DMA8000, PerkinElmer, USA) was used in the bending mode, ranging from room temperature to 250 °C at a heating rate of 5 °C/min and a frequency of 1 Hz.

RESULTS AND DISCUSSION

Synthesis and Characterization of APPN

The synthetic route of the APPN compound is illustrated in Fig. 1.

According to the FTIR spectrum of APPN (Fig. 2a), the absorption band at 2223 cm^{-1} corresponds to the nitrile group, confirming the phthalonitrile moiety in 3-aminophenoxyphthalonitrile. The most important structural modification of 3-aminophenoxyphthalonitrile, compared to 4-nitrophthalonitrile, is the introduction of an amino group. This was verified by the appearance of primary amine peaks at 3448 and 3365 cm^{-1}. Furthermore, the absorption peak at 1251 cm^{-1} confirmed the formation of an aryl ether group. Based on these wavenumbers, it can be concluded that APPN was successfully synthesized.

Further characterization of APPN was performed by ^{1}H-

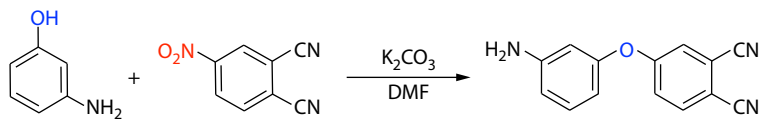

Fig. 1 The synthesis route for APPN.

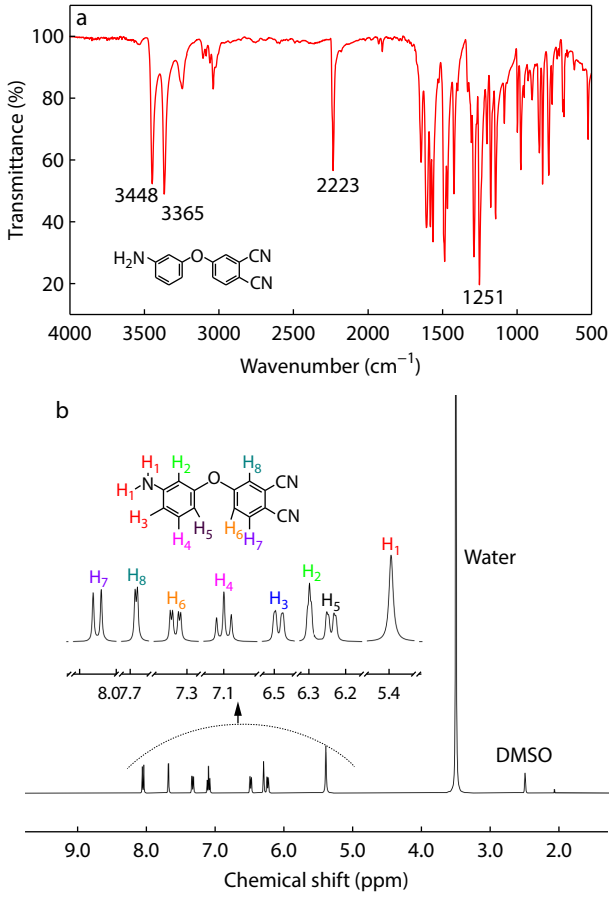

Fig. 2 (a) FTIR spectrum and (b) ^{1}H-NMR spectrum for the APPN.

NMR spectroscopy. As shown in Fig. 2(b), aromatic protons adjacent to the two cyano groups were observed in the downfield regions because of the inductive and resonance effects of the cyano and ether groups. The H_8 proton was observed at 7.65 ppm. The H_7 proton appears at 8.05 ppm, which is attributed to ortho-coupling. The signal corresponding to H_6 appears at 7.3 ppm, arising from ortho-coupling with its neighboring proton. The resonance effects of the cyano groups have a stronger influence on H_7 and H_8 because they are in closer proximity than H_6.

The aromatic protons adjacent to the primary amine group are shifted upfield relative to those influenced by the cyano groups owing to the electron-donating and resonance effects of the amino substituent. The chemical shift of the H_2 proton appears at 6.3 ppm, corresponding to ortho-coupling with an adjacent amino group. The H_3 proton was observed at 6.5 ppm as a doublet owing to coupling with two ortho-positioned neighbors. The H_5 Proton appears at 6.2 ppm as a doublet peak. In addition, the H_1 protons, which were attached to the nitrogen atom, appeared as a broad signal at 5.4 ppm.

Synthesis and Characterization of MPN Monomer

The synthesis of the MPN monomer is illustrated in Fig. 3. In the first step, the APPN reagent reacts with maleic anhydride in the presence of potassium carbonate to form the amic acid intermediate. Subsequently, amic acid undergoes an intramolecular cyclization reaction, yielding the desired MPN monomer.

According to the FTIR spectrum of the synthesized monomer (MPN) (Fig. 4a), the absorption bands at 698 and 828 cm^{-1} corresponded to the bending vibrations of the maleimide C—H bonds, indicating the formation of the maleimide moiety in the monomer structure. Additionally, the peak observed at 3101 cm^{-1} was attributed to the stretching vibrations of the maleimide double bond, further confirming the presence of the maleimide group. The absorption band at 1147 cm^{-1} corresponds to the C—N bond within the maleimide ring, which is clearly visible in the FTIR spectrum of the monomer. Moreover, the peaks at 1717 and 1776 cm^{-1} were assigned to the stretching vibrations of the imide carbonyl groups, providing strong evidence for the successful synthesis of the maleimide moiety.

The cyanide groups present in the monomer are observed at 2223 cm^{-1}, confirming the presence of the phthalonitrile segment within the monomer structure.

According to Fig. 4(b), which presents the ^{1}H-NMR spectrum of the MPN compound, the H_7 proton appears at a higher chemical shift than the other protons and is observed as a doublet at 8.1 ppm. This splitting arises from the anisotropic effect and electron density surrounding this proton. The signals of protons H_8, H_1, and H_2 overlapped and appear at 7.8 ppm. The H_4 proton appeared as a well-resolved triplet at 7.6 ppm, attributable to its neighboring protons H_6 and H_5. The H_9 proton also appeared as a doublet at 7.5 ppm, split by H_7. The H_5 proton is observed as a doublet at a chemical shift of 7.3 ppm, split by H_4. The H_3 proton resonates at 7.2 ppm, and finally, the H_6 proton is clearly observed at 7.15 ppm in the spectrum.

Fig. 5 shows the ^{13}C-NMR of the MPN monomer. As shown

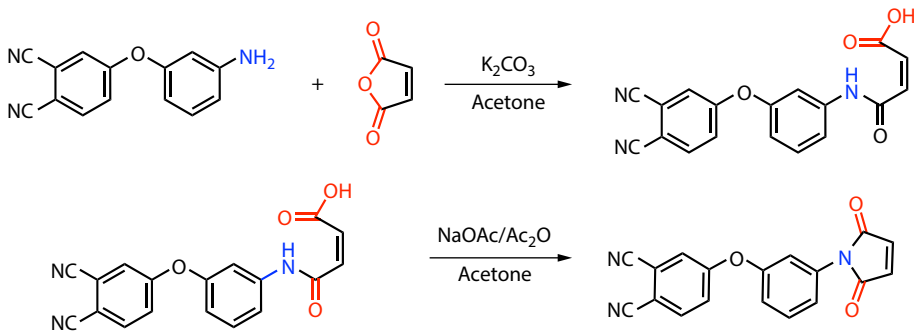

Fig. 3 Synthesis route of MPN monomer.

https://doi.org/10.1007/s10118-026-3798-z

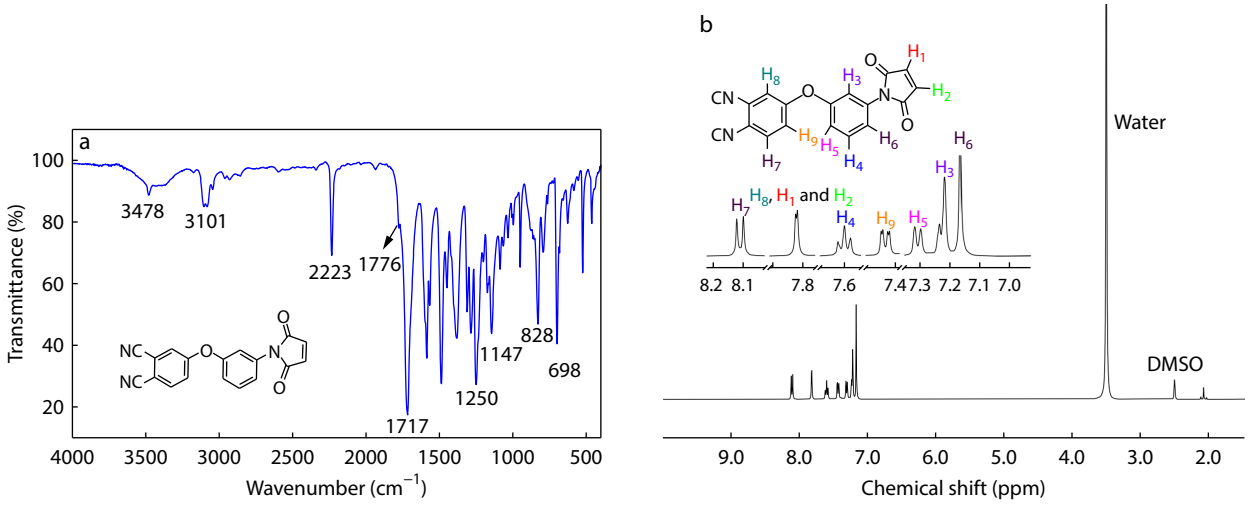

Fig. 4 (a) FTIR spectrum and (b) ^{1}H-NMR spectrum of MPN monomer.

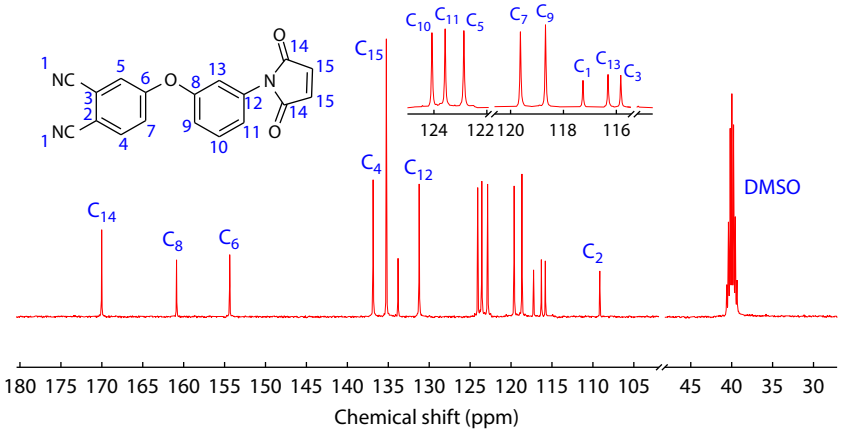

Fig. 5 ^{13}C-NMR spectrum of MPN monomer.

in Fig. 5, this resin has some characteristic peaks, such as carbonyl groups, double bonds, and CN functional groups. In the ^{13}C-NMR spectrum, C_{14} appeared at a chemical shift of 170 ppm, which is characteristic of a carbonyl group, thereby confirming the presence of this functional group in the monomer structure. C_8 and C_6, which are not directly bonded to protons, resonated at 160 and 150 ppm, respectively. C_4 appears at a relatively higher chemical shift than the other carbons, which can be attributed to the electron-withdrawing effect of the cyano groups. C_{15}, owing to the presence of a double bond, resonates at 135 ppm, which is a characteristic region for double-bonded carbons and confirms the presence of the maleimide moiety in the structure. The remaining signals are shown in Fig. 5, further supporting the successful formation of the MPN monomer.

The results of the CHN elemental analysis of the MPN monomer are presented in Table 2. The molecular formula of the MPN monomer is $C_{18}H_9N_3O_3$ and it has a molecular weight of 315 g/mol. The calculated C, H, N, and O contents in the MPN monomer were 68.62%, 2.88%, 13.33%, and 19.23%, respectively. Based on the CHN elemental analysis, the actual values of C, H, N, and O are 65.33%, 2.85%, 12.63%, and 15.23%, respectively. A comparison of the theoretical and experimental values for the C, H, N, and O percentages indicates the successful synthesis of the MPN monomer.

Table 2 CHN analysis for MPN monomer.

Element	C (%)	H (%)	N (%)	O (%)
Theoretical value	68.62	2.88	13.33	19.23
Experimental value	65.33	2.85	12.63	15.23

Curing Behavior and Curing Mechanism of MPN with DABA Curing Agent

The curing reaction between the DABA and MPN is shown in Fig. 6. The allylic part of DABA undergoes an Ene-Alder reaction with the maleimide part of MPN. After the reaction was complete, the cyanide group of the MPN resin participated in the curing process, yielding phthalocyanine.

DSC analysis (Fig. 7a) of the neat synthesized monomer (MPN) provides valuable insight into its thermal behavior and curing mechanism. The first endothermic transition observed at 106.8 °C corresponds to the melting of the monomer, indicating good processability and confirming that the monomer exists in a crystalline state at room temperature with fusion enthalpy of 51.2 J/g. Such a relatively low melting point is advantageous because it enables the efficient impregnation of reinforcing fibers and uniform resin flow during composite fabrication. Conventional phthalonitrile monomers are char-

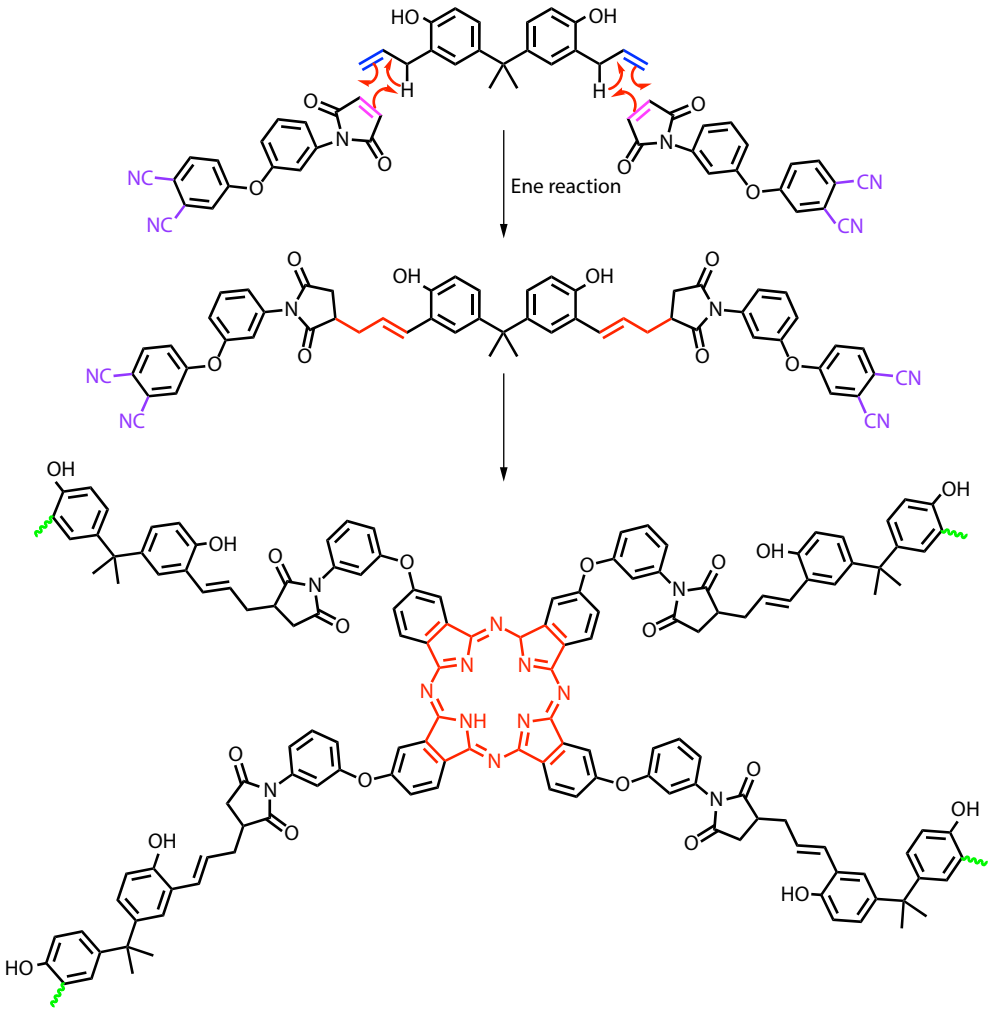

Fig. 6 Curing reaction between DABA and MPN monomer.

acterized by high crystalline melting temperatures, typically exceeding 180 °C, which is close to their polymerization onset temperature. This limitation forces processing into a very narrow thermal window, which severely limits its practical applications. In contrast, the DSC thermogram for the MPN monomer shows the first endothermic melting transition at 106.8 °C, which is significantly lower than that of standard phthalonitriles. This substantial melting-point depression arises from molecular design; the incorporation of the maleimide moiety disrupts the molecular symmetry and reduces the crystalline packing efficiency.

Upon further heating, a distinct exothermic peak centered at 304.9 °C was observed with enthalpy of −157.9 J/g, which can be attributed to the radical homopolymerization of the maleimide double bonds. This reaction leads to the formation of succinimide structures, which serve as the first-stage curing network within the dual-curing system. The temperature of this exothermic event aligns well with reported data for maleimide-based systems, confirming that the initial curing step predominantly involves maleimide addition reactions.

Interestingly, a second exothermic peak at 331.4 °C was detected with an enthalpy of −170.2 J/g, signifying the onset of phthalonitrile polymerization. The occurrence of this secondary polymerization in the absence of an external catalyst implies that the system exhibits autocatalytic behavior. This phenomenon can be explained by considering the partial thermal decomposition of the succinimide structures formed during maleimide polymerization. Previous studies,[50,51] have demonstrated that succinimide groups can undergo minor degradation at approximately 300 °C, generating trace quantities of amine species. Although the extent of this decomposition is limited, even small amounts of liberated amines act as strong nucleophilic initiators for phthalonitrile trimerization.

A comparison of the processing temperatures of the Maleimide-containing phthalonitrile dual-curing resin systems is listed in Table 3.

The dual exothermic transitions summarized in Table 4 clearly illustrate this two-step curing mechanism: (1) maleimide homopolymerization, forming a pre-crosslinked intermediate, and (2) phthalonitrile self-polymerization, induced by thermally generated amines, leading to a highly aromatic, crosslinked network. This mechanism not only explains the autocatalytic behavior observed in DSC but also highlights the chemical synergy between the maleimide and

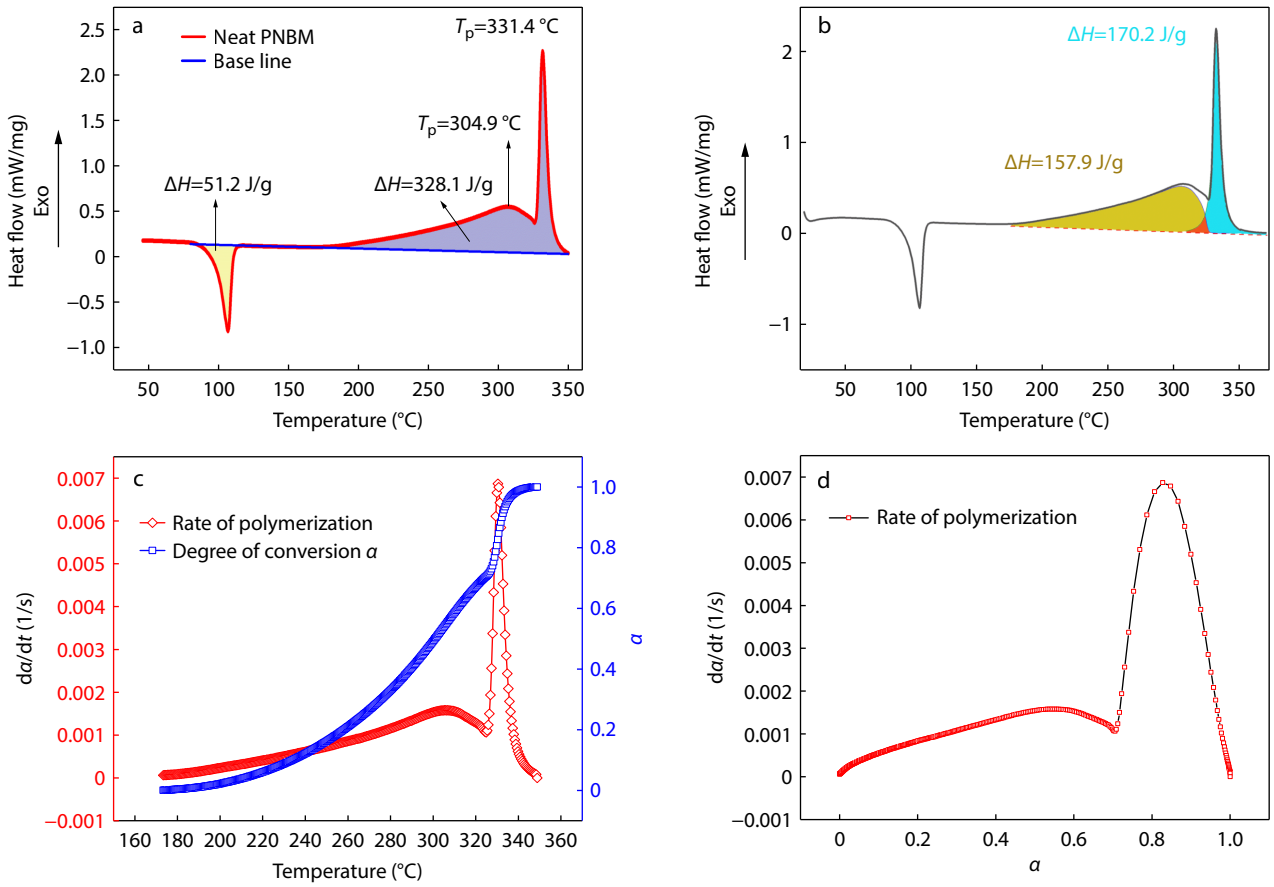

Fig. 7 (a) The DSC curve of the monomer in the absence of a curing agent; (b) Enthalpy of curing based on maleimide and phthalonitrile part; (c) Degree of conversion and rate of polymerization versus temperature; (d) The rate of polymerization versus degree of conversion.

Table 3 Processing windows of reported different MPN monomers.

Structure	Melting temp. (°C)	First curing temp. (°C)	Second curing temp. (°C)	Ref.
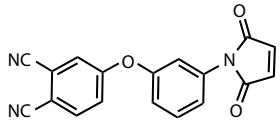	106.8	304.9	331.4	This work and [48]
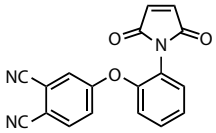	200.8	278.9	342.8	[48]
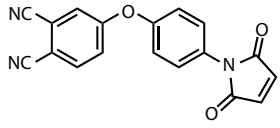	210.4	287.9	329.9	[48]
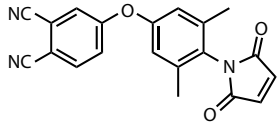	149.0	–	348.0	[52]
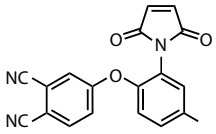	143	315	347	[52]

Table 4 DSC results of neat MPN monomer.

Sample parts	T_i (°C)	T_p (°C)	ΔH (J/g)
Maleimide part	211.4	304.9	−157.9
Phthalonitrile part	325.9	331.4	−170.2

phthalonitrile functionalities within the MPN structure (Fig. 7b).

Kinetic analysis (Fig. 7c) provides quantitative insight into the reaction mechanism. The degree of conversion (α) initially increased slowly up to approximately 270 °C, followed by a rapid acceleration between 280–330 °C, coinciding with the onset of maleimide polymerization. The rate of polymerization ($d\alpha/dt$) reaches a maximum at about 310 °C, corresponds to the point where radical concentration and mobility are optimal. Beyond this temperature, the rate decreased because of the diffusion-controlled nature of the reaction as the system was cross-linked. A secondary increase in the conversion rate was observed near 330–340 °C, confirming the self-catalyzed polymerization of the phthalonitrile fragments, likely promoted by trace amine species generated from the minor decomposition of succinimide structures around 300 °C.

The plot of the rate of polymerization versus the degree of conversion (Fig. 7d) exhibits the characteristic autocatalytic behavior of thermosetting systems, where the rate increases with conversion up to a critical point ($\alpha \approx 0.55$) before decreasing sharply as network rigidity restricts molecular motion. This kinetic profile supports the presence of a dual-curing mechanism, with the maleimide segment initiating network formation and the phthalonitrile component subsequently contributing to high-temperature crosslinking.

To ensure complete curing of the phthalonitrile resin with DABA as the curing agent and to define an appropriate curing cycle, a sample containing 21 wt% DABA was cured at three temperatures (200, 315, and 350 °C) for different durations. The curing process was monitored using FTIR spectroscopy to observe the decrease in nitrile group intensity and the increase in the intensities of isoindoline, triazine, and phthalocyanine groups, indicating the progress of curing.

As shown in Fig. 8, the absorption bands at 700 and 830 cm^{-1}, attributed to out-of-plane bending vibrations of the =C—H group of the maleimide moiety, gradually decreased in intensity during the curing process, indicating curing of the maleimide group. Moreover, the gradual reduction in the peak at 2223 cm^{-1}, corresponding to cyanide group stretching vibrations, demonstrates progressive curing of the phthalonitrile group.

To calculate the DOC, Eq. (1) was used for the two reactive parts of MPN, maleimide, and cyanide, and the results are shown in Fig. 9. The maleimide part (blue dashed curve) exhibits a higher degree of conversion at lower temperatures (around 200–315 °C), which aligns with the well-documented radical polymerization behavior of maleimide groups. The curing of this group progressed rapidly during the initial stage, reaching approximately 95% completion at 350 °C. In contrast, the phthalonitrile part (green dashed curve) demonstrated a delayed curing, with significant advancement only above 300 °C. This behavior is consistent with the high activation energy required for phthalonitrile trimerization and the formation of thermally stable heterocyclic networks.[53]

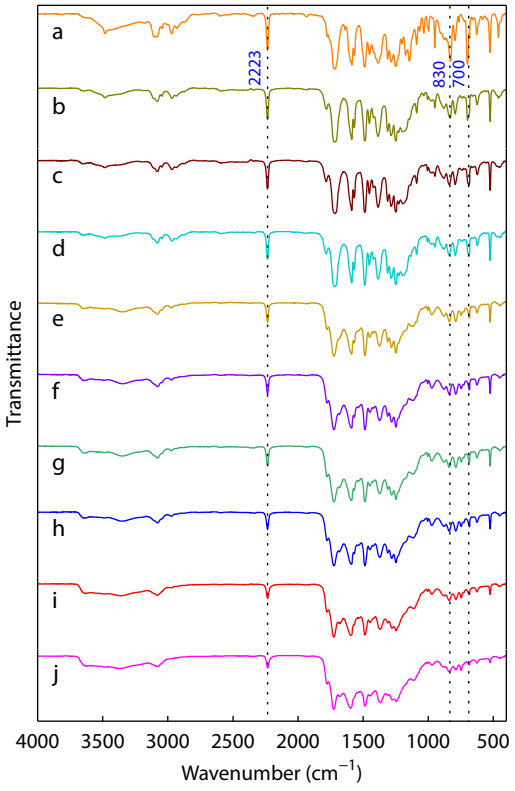

Fig. 8 FTIR spectra of MPN resins during the curing process. (a) Before curing, (b) 30 min @ 200 °C, (c) 1 h @ 200 °C, (d) 2 h @ 200 °C, (e) 2 h @ 200 °C + 4 h @ 315 °C, (f) 2 h @ 200 °C + 6 h @ 315 °C, (g) 2 h @ 200 °C + 8h @ 315 °C, (h) 2h @ 200°C + 10 h @ 315 °C, (i) 2 h @ 200 °C + 10 h @ 315 °C + 2 h @ 350 °C, (j) 2 h @ 200 °C + 10 h @ 315 °C + 6 h @ 350 °C.

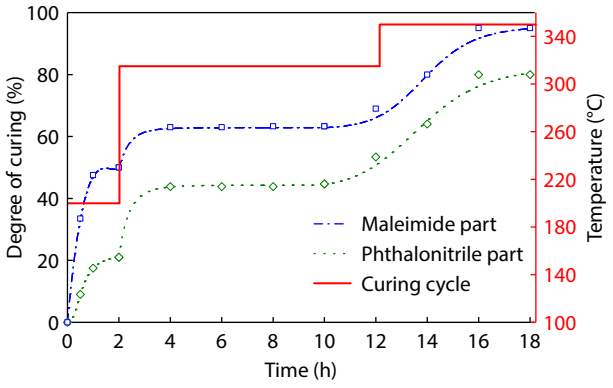

Fig. 9 Curing cycle and degree of curing of MPN with the presence of DABA curing agent.

Mechanical and Thermal Properties of MPN/DABA/Carbon Fiber Composites

The interlaminar shear strength (ILSS) results of the MPN/DABA/carbon fiber composite directly reflect the influence of the curing cycle on the degree of crosslinking and the resulting mechanical properties of the composite of the resin matrix and carbon fibers. As shown in Table 5, three distinct curing cycles were applied to cure the MPN/DABA/carbon fiber composite to investigate the effect of curing cycles on the me-

chanical properties of the dual-curing MPN resin.

The ILSS results are shown in Fig. 10. In the MPN-DABA 200 sample cured for only 30 min at 200 °C, the ILSS value of 25 MPa indicates incomplete polymerization of both reactive sites. At this temperature and short curing time, only limited addition reactions occurred in the maleimide domains, whereas the phthalonitrile moieties remained largely unreacted. Consequently, the matrix exhibited a relatively low crosslink density and weaker fiber-matrix adhesion, leading to a lower shear strength.

Table 5 Different curing cycles applied for curing of MPN/DABA/carbon fiber composite.

Sample code	Curing cycle
MPN-DABA 200	30 min @ 200 °C
MPN-DABA 315	2 h @ 200 °C + 4 h @ 315 °C
MPN-DABA 350	2 h @ 200 °C + 4 h @ 315 °C + 6 h @ 350 °C

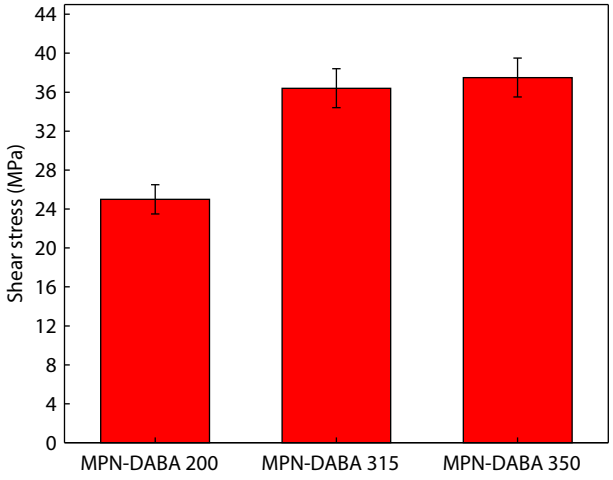

Fig. 10 ILSS values for MPN-DABA systems.

In the MPN-DABA 315 sample cured for 2 h at 200 °C followed by 4 h at 315 °C, the ILSS increased to 36.4 MPa. According to the FTIR results, approximately 63% of maleimide and 43.8% of phthalonitrile groups were cured. At this stage, the polymer network became more integrated as the maleimide units underwent further addition polymerization, and partial phthalonitrile curing began. The enhanced crosslinking improves matrix rigidity and fiber-matrix bonding, although the incomplete polymerization of the phthalonitrile units still limits the overall load transfer efficiency.

The MPN-DABA 350 sample, which underwent the most extensive curing cycles, achieved the highest ILSS value of 37.5 MPa. At these elevated temperatures, nearly 95% of maleimide and 80% of phthalonitrile segments were converted. The formation of a highly crosslinked aromatic heterocyclic network significantly enhances the matrix modulus and thermal stability. Moreover, the improved crosslink density reduces the mobility of the polymer chains at the interface, thereby increasing the frictional resistance to interlaminar shear and preventing microcrack propagation under loading. The incremental increase in ILSS with progressive curing demonstrated a clear correlation between the degree of cure and mechanical integrity. Complete polymerization of the maleimide phase establishes a rigid backbone, whereas advanced phthalonitrile crosslinking contributes to high thermal resistance and mechanical strength. The overall ILSS values fell within the expected range for phthalonitrile- and bismaleimide-based composites, confirming that the synthesized MPN-DABA resin system achieved a mechanical performance intermediate between those of conventional BMI and phthalonitrile matrices. Table 6 compares the ILSS values reported in the literature for composites based on the PN

Table 6 Reported ILSS values for PN resins composites in the literature.

Structure	Fiber type	ILSS value (MPa)	Ref.
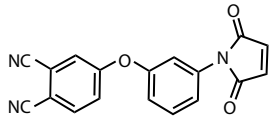	Carbon Fiber	37.5	This work
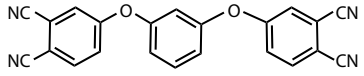	Quartz Fiber	30.0	[54]
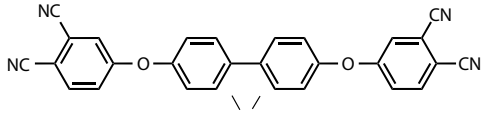	Glass Fiber	44.0	[55]
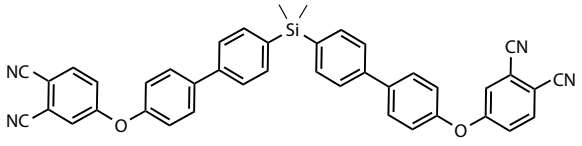	Quartz Fiber	30.0	[56]
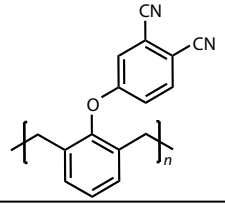	Carbon Fiber	30.6	[57]

https://doi.org/10.1007/s10118-026-3798-z

resins. [54–57]

DMTA analysis provides critical insight into the viscoelastic behavior and degree of curing of the synthesized MPN-DABA resin system. As illustrated in Fig. 11, the MPN-DABA 200 sample exhibited a glass transition temperature below 100 °C, a value which was markedly lower than fully cured phthalonitrile and bismaleimide resins. This substantial reduction in T_g directly reflects the insufficient crosslinking density of the polymer matrix owing to incomplete curing reactions under the mild thermal conditions applied (30 min at 200 °C). It should also be noted that the composite exhibited a relatively high storage modulus, even under incomplete curing, up to temperatures close to 100 °C. This behavior indicates that a partially crosslinked network was already formed during the early stages of curing, providing sufficient stiffness and dimensional stability to the material before full curing occurred.

From a molecular perspective, the low T_g indicates that the polymer chains remain highly mobile, suggesting the predominance of unreacted or partially reacted maleimide and phthalonitrile moieties. The FTIR analysis confirmed this interpretation, revealing that only approximately 30% of the maleimide double bonds and approximately 9% of the phthalonitrile groups underwent conversion during the initial curing stage (Fig. 9). Such limited reaction extents are expected, as maleimide addition polymerization can initiate at moderate temperatures, whereas phthalonitrile curing requires substantially higher activation energies, typically occurring above 300 °C. Consequently, the polymer network at this stage was dominated by a loosely crosslinked maleimide structure with minimal phthalonitrile contribution, resulting in a soft, low-modulus matrix.

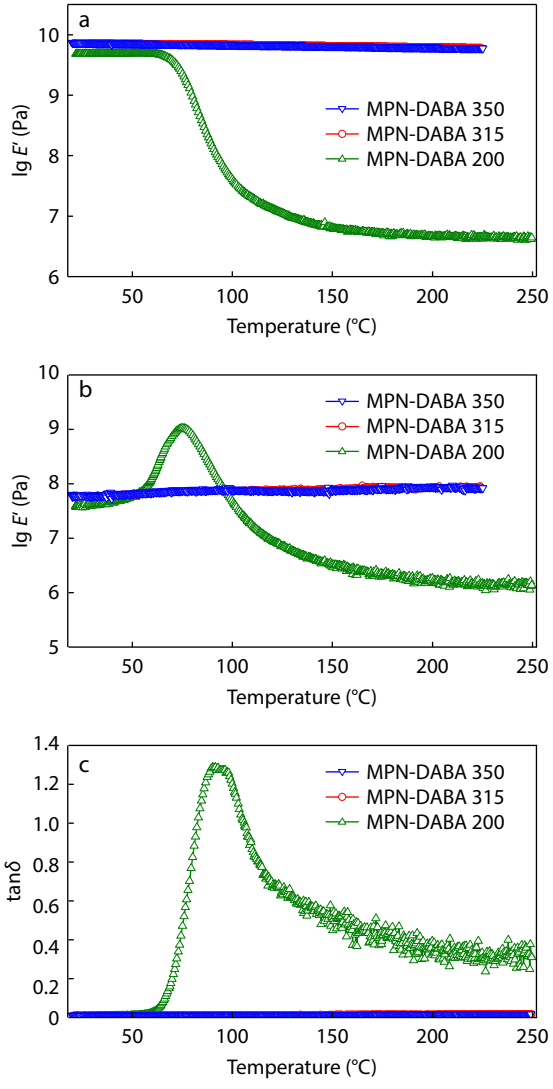

Fig. 11 DMTA curves for composites cured with the different curing cycles: (a) storage modulus, (b) loss modulus and (c) tanδ.

The results conclusively demonstrate that under these conditions, phthalonitrile curing remains largely inactive, confirming the stepwise curing behavior of the dual-curing MPN resin. This finding aligns with the observed FTIR data, which show that the degree of maleimide conversion is approximately three times higher than that of the phthalonitrile monomer, reflecting the inherently distinct thermal reactivity of the two functional groups.

Further comparison with the DMTA profiles of MPN-DABA 315 and MPN-DABA 350 revealed a systematic shift in T_g toward higher temperatures with increasing curing temperature and duration. This shift signifies progressive network formation through the simultaneous completion of maleimide addition reactions and the onset of phthalonitrile trimerization and ring closure, leading to a denser aromatic structure with reduced chain mobility. The disappearance of T_g within the 25–250 °C range for these advanced composites indicates that the glass transition has moved beyond the measurable window, confirming the formation of a highly crosslinked, thermally stable polymer. To provide a better understanding of the intrinsic properties of the MPN/DABA matrix, the thermomechanical and thermal properties of the corresponding neat resin previously reported in the literature[48] are summarized in Table 7. As shown, the neat MPN/DABA resin exhibited a high glass transition temperature (T_g) of 368.4 °C, indicating the formation of a highly crosslinked polymer network with excellent thermal resistance. DMTA further revealed a storage modulus of 4243 MPa at room temperature, which remained as high as 2521 MPa at 300 °C, indicating remarkable retention of stiffness at elevated temperatures.

The neat resin also exhibited satisfactory mechanical per-

Table 7 Thermo-mechanical and thermal properties of the neat MPN/DABA resin.[48]

Property	Value
T_g (°C)	368.4
E' at room temperature (MPa)	4243
E' at 300 °C (MPa)	2521
Flexural strength (MPa)	90
Flexural modulus (GPa)	4.38
Impact strength (kJ/m^2)	11.81
$T_{5\%}$ in N_2 (°C)	456
$T_{10\%}$ in N_2 (°C)	505
Char yield in N_2 (%)	75.9
$T_{5\%}$ in air (°C)	458.8
$T_{10\%}$ in air (°C)	507.9

formance with a flexural strength of 90 MPa, flexural modulus of 4.38 GPa, and impact strength of 11.81 kJ/m^2. TGA demonstrated excellent thermal stability under both nitrogen and air atmospheres. Under nitrogen, the temperatures corresponding to 5% and 10% weight losses were 456 and 505 °C, respectively, with a char yield of 75.9%. Similarly, in air, the $T_{5\%}$ and $T_{10\%}$ values reached 458.8 and 507.9 °C, respectively, confirming the outstanding thermal stability of the cured MPN/DABA resin. These data provide the intrinsic thermomechanical characteristics of the MPN/DABA matrix and support the interpretation of the composite results presented herein. The high thermal stability and stiffness of the neat resin indicate that the observed performance of the carbon fiber-reinforced composites originates not only from the reinforcing effect of the carbon fibers but also from the excellent inherent properties of the MPN/DABA matrix.

To further investigate the thermal properties of the MPN/DABA/carbon fiber composite, TGA was performed on the MPN-DABA 350 sample. The selection of MPN-DABA 350 for thermal analysis was based on its superior mechanical and thermal performances, as demonstrated by the ILSS and DMTA analyses, respectively, which indicated that the optimized curing cycle resulted in a well-developed crosslinked structure. The high degree of curing (approximately 95% for the maleimide segment and 80% for the phthalonitrile segment) strongly indicates that this sample possesses a robust three-dimensional polymer network, making it a suitable candidate for evaluating the thermal behavior *via* TGA (Fig. 12).

As shown in the corresponding Fig. 12, the initial decomposition temperature (T_{id}) for this system was approximately 340 °C, while the final decomposition temperature (T_{fd}) occurs at 675 °C. T_{id} represents the onset of significant mass loss, which corresponds to the initial cleavage of thermally unstable groups within the polymer network. In this temperature range, minor degradation of aliphatic linkages, residual solvent removal, or partial scission of less stable succinimide structures may occur. This initial event signifies the transition from thermal stability to the beginning of the polymer backbone degradation. T_{fd} marks the completion of decomposition, which corresponds to the breakdown of the highly aromatic crosslinked network formed during the final curing stage. This elevated decomposition limit is characteristic of phthalonitrile-derived polymers, which decompose through stepwise bond scission and carbonization rather than rapid

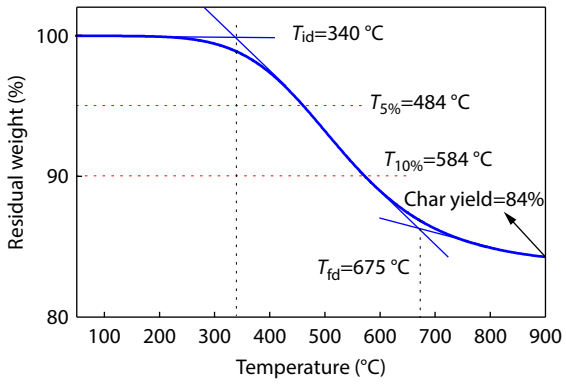

Fig. 12 TGA curve of the MPN-DABA 350 composite.

volatilization. The high T_{fd} value, combined with the substantial char residue observed beyond this temperature, confirms the formation of a thermally stable carbon structure upon heating, indicative of efficient crosslinking and a high aromatic content within the polymer backbone. As shown in Table 8, the $T_{5\%}$ of the MPN-DABA 350/carbon fiber composite was slightly lower than that of the pure phthalonitrile-based composite,[58] yet approximately 80 °C higher than that of the bismaleimide-based composite.[23] This observation can be rationalized in terms of the chemical structure of the MPN resin. The incorporation of maleimide groups introduces aliphatic linkages that may begin to thermally degrade at relatively lower temperatures than the highly aromatic phthalonitrile framework, thereby slightly reducing the onset of the weight loss. Nevertheless, the presence of the phthalonitrile backbone imparts considerable thermal resistance through the formation of stable triazine and isoindoline structures during curing, which effectively elevates the overall decomposition temperature compared with BMI systems.

Table 8 TGA results of MPN, PN, and BMI with carbon fiber.

Sample	Argon atmosphere		
	$T_{5\%}$ (°C)	$T_{10\%}$ (°C)	Char yield at 900 °C (%)
MPN/Carbon fiber	484	584	84
PN/Carbon fiber	502	597	87
BMI/Carbon fiber	407	423	37

The char yield at 900 °C, which shows only a 3% reduction relative to the phthalonitrile-based composite, but a substantial improvement over the BMI-based system, further supports the formation of a highly condensed aromatic structure upon pyrolysis. The high char residue indicates efficient carbonization and suggests that the polymer network retains significant aromatic character despite the inclusion of the maleimide units. This behavior is consistent with the thermally stable crosslinked structures typically observed in phthalonitrile systems, where extensive cyclization and ladder-type structures contribute to the excellent thermal resistance.

From a structural chemistry perspective, the synthesized phthalonitrile monomer containing a maleimide group represents a rational design that bridges the processing advantages of BMI resins, such as a lower curing temperature and improved flowability, with the superior thermal stability of the phthalonitrile networks. The introduction of maleimide moieties lowers the initial curing temperature by promoting addition reactions at lower activation energies, thereby widening the processing window and enhancing manufacturability without compromising the high-temperature performance.

CONCLUSIONS

In this study, a maleimide-functionalized phthalonitrile monomer (MPN) with a melting point of 106.8 °C was successfully synthesized, offering improved processability over conventional phthalonitriles. DSC analysis confirmed that the resin could polymerize autocatalytically, while FTIR results guided the design of an optimized dual-stage curing cycle using 21 wt% DABA as a curing agent. The curing schedule affected the me-

https://doi.org/10.1007/s10118-026-3798-z

chanical and thermal properties of the fabricated composites. As the curing progressed, the formation of a highly crosslinked aromatic heterocyclic network markedly enhanced the matrix modulus and thermal stability. The increased degree of crosslinking further improved the matrix rigidity and the fiber-matrix interfacial bonding.

Mechanical testing revealed that increasing the curing degree significantly enhanced interlaminar shear strength (ILSS) of the fully cured MPN-DABA 350 sample. DMTA analysis showed a corresponding increase in T_g, confirming the formation of a highly crosslinked network. The DMTA results demonstrate that the composite exhibits strong thermal-mechanical stability, efficient energy dissipation behavior, and effective curing evolution, leading to a well-developed crosslinked polymer structure. The TGA results demonstrate excellent thermal stability, indicating a thermally robust aromatic structure. Overall, the synthesized MPN/DABA composite exhibited intermediate thermal and mechanical properties between those of the traditional bismaleimide and phthalonitrile systems. This hybrid design effectively combines the ease of processing BMI resins with the thermal endurance of phthalonitriles, making it a promising candidate for high-temperature structural and aerospace applications.

Conflict of Interests

The authors declare no interest conflict.

Data Availability Statement

The data are available from the corresponding author upon reasonable request.

REFERENCES

1 Liu, J.; Wang, S.; Peng, Y.; Zhu, J.; Zhao, W.; Liu, X. Advances in sustainable thermosetting resins: from renewable feedstock to

Graphical Abstract

The Effect of Curing Cycle on Interlaminar Shear Strength and Thermal Properties of Carbon Fiber Composite of High Temperature Maleimide-containing Phthalonitrile Dual-curing Resin

Hassan Fattahi, Milad Hatami, Mohammad Reza Ehsani, and Mehrzad Mortezaei

Malek Ashtar University of Technology, Iran

A low-melting maleimide-functional phthalonitrile was synthesized, and the effects of different curing cycles on the ILSS and thermal properties of its composite with carbon fibers were investigated. The optimized composite exhibited an ILSS of about 37.5 MPa, high storage modulus, and excellent thermal stability with $T_{5\%}$=484 °C, $T_{10\%}$=584 °C, and 84% char yield at 900 °C.

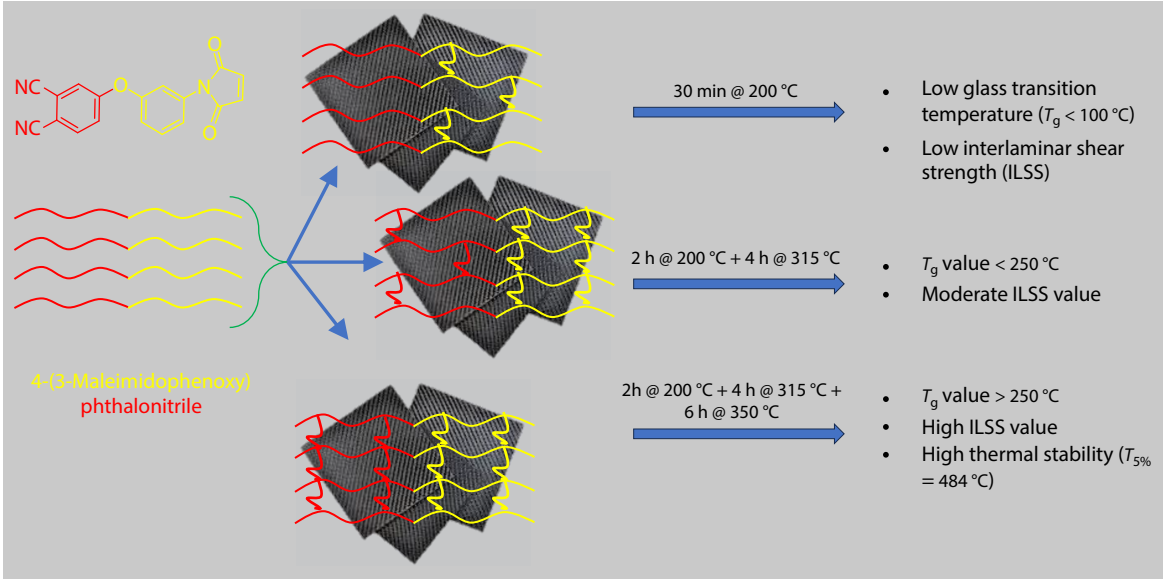

Chinese J. Polym. Sci., 2026 *https://doi.org/10.1007/s10118-026-3798-z*

high performance and recyclability. *Prog. Polym. Sci.* **2021**, *113*, 101353.
2 Huang, X.; Peng, S.; Zheng, L.; Zhuo, D.; Wu, L.; Weng, Z. 3D printing of high viscosity UV-curable resin for highly stretchable and resilient elastomer. *Adv. Mater.* **2023**, *35*, 2304430.
3 Sun, X.; Wang, S.; Dong, S.; Chen, X.; Dong, X.; Wang, Y.; Jian, X.; Liu, C. Synthesis and degradation mechanisms of Schiff-base-containing phthalonitrile resins: thermal stability and bond reconfiguration. *Polym. Degrad. Stab.* **2026**, *246*, 111945.
4 Gacal, B.; Cianga, L.; Agag, T.; Takeichi, T.; Yagci, Y. Synthesis and characterization of maleimide (co)polymers with pendant benzoxazine groups by photoinduced radical polymerization and their thermal curing. *J. Polym. Sci. Part A: Polym. Chem.* **2007**, *45*, 2774–2786.
5 Sirotin, I. S.; Sarychev, I. A.; Vorobyeva, V. V.; Kuzmich, A. A.; Bornosuz, N. V.; Onuchin, D. V.; Gorbunova, I. Y.; Kireev, V. V. Synthesis of phosphazene-containing, bisphenol A-based benzoxazines and properties of corresponding polybenzoxazines. *Polymers* **2020**, *12*, 1225.
6 Xu, M.; Lei, Y.; Ren, D.; Chen, L.; Li, K.; Liu, X. Thermal stability of allyl-functional phthalonitriles-containing benzoxazine/bismaleimide copolymers and their improved mechanical properties. *Polymers* **2018**, *10*, 596.
7 Jahani, M.; Fatahi, H.; Mortezaeei, M. Effect of aromatic amine structure as a curing agent on molecular packing and mechanical properties of cured epoxy resin. *Iran. J. Polym. Sci. Technol.* **2019**, *32*, 267–276 (in Persian).
8 Hajebi, S.; Payamani, M.; Fattahi, H.; Mortezaei, M.; Jalilolghadr, S. Dual-curing epoxy thermosets: Design, curing, properties and applications. *Polym. Rev.* **2025**, *65*, 250–280.
9 Pouladvand, A. R.; Mortezaei, M.; Fattahi, H.; Amiri Amraei, I. A novel custom-tailored epoxy prepreg formulation based on epoxy-amine dual-curable systems. *Compos. Part A Appl. Sci. Manuf.* **2020**, *132*, 105852.
10 Nechausov, S. S.; Bulgakov, B. A.; Solopchenko, A. V.; Serdan, A. A.; Kalugin, D. I.; Lyalin, A.; Kepman, A. V.; Malakho, A. P. Thermosetting matrices for composite materials based on allyl/propargyl substituted novolac resins. *J. Polym. Res.* **2016**, *23*, 114.
11 Augustine, D.; Mathew, D.; Nair, C. P. R. One component propargyl phthalonitrile novolac: synthesis and characterization. *Eur. Polym. J.* **2015**, *71*, 389–400.
12 Nechausov, S.; Bulgakov, B.; Kalugin, D.; Babkin, A.; Kepman, A.; Malakho, A.; Avdeev, V. Carbon fabric reinforced addition-cure phenolic resins based on propargyl and allyl ether functional novolac produced by vacuum infusion. *Eurasian Chem.-Technol. J.* **2020**, *22*, 99–106.
13 Bulgakov, B.; Babkin, A.; Makarenko, I.; Tikhonov, N.; Kalugin, D.; Kepman, A.; Malakho, A.; Avdeev, V. Ni(II) and Cu(II) based catalysts for propargylated novolac resins curing: Activity study and curing process simulation. *Eur. Polym. J.* **2015**, *73*, 247–258.
14 Dirlikov, S. K. Propargyl-terminated resins—a hydrophobic substitute for epoxy resins. *High Perform. Polym.* **1990**, *2*, 67–77.
15 Bulgakov, B.; Kalugin, D.; Babkin, A.; Makarenko, I.; Malakho, A.; Kepman, A.; Avdeev, V.; Garadja, N.; Rogozin, A. Propargylated novolac resins for fibre-reinforced plastics: processing aspects. *Can. J. Chem. Eng.* **2016**, *94*, 46–52.
16 Hamerton, I. High-performance thermoset-thermoset polymer blends: A review of the chemistry of cyanate ester–bismaleimide blends. *High Perform. Polym.* **1996**, *8*, 83–95.
17 Bauer, J.; Bauer, M. Curing of cyanates with primary amines. *Macromol. Chem. Phys.* **2001**, *202*, 2213–2220.
18 Uhlig, C.; Kahle, O.; Schäfer, O.; Ewald, D.; Oswaldbauer, H.; Bauer, J.; Bauer, M. Blends of tri-block copolymers and addition curing resins: Influence of block copolymer–resin compatibility on toughness and matrix properties on toughenability. *React. Funct. Polym.* **2019**, *142*, 159–182.
19 Ahmadi, M.; Fattahi, H.; Mortezaei, M.; Mirbagheri, S. M. J. High temperature cyanate ester/carbon fiber composite with high ILSS based on synthesized 2,2′-bis(4-cyanatophenyl) propane resin. *J. Sci. Technol. Compos.* **2024**, *11*, 2419–2428 (in Persian).
20 Iredale, R. J.; Ward, C.; Hamerton, I. Modern advances in bismaleimide resin technology: a 21st century perspective on the chemistry of addition polyimides. *Prog. Polym. Sci.* **2017**, *69*, 1–21.
21 Dolci, E.; Froidevaux, V.; Joly-Duhamel, C.; Auvergne, R.; Boutevin, B.; Caillol, S. Maleimides as a building block for the synthesis of high performance polymers. *Polym. Rev.* **2016**, *56*, 512–556.
22 Evsyukov, S.; Klomp-de Boer, R.; Stenzenberger, H. D.; Pohlmann, T.; ter Wiel, M. A new m-xylylene bismaleimide-based high performance resin for vacuum-assisted infusion and resin transfer molding. *J. Compos. Mater.* **2019**, *53*, 3063–3072.
23 Payamani, M.; Fattahi, H.; Mortezaei, M. Synthesis and characterization of 4,4′-bis(maleimido)diphenylmethane resin and evaluation of its curing behavior in blending with epoxy. *Iran. J. Polym. Sci. Technol.* **2022**, *35*, 339–352 (in Persian).
24 Keller, T. M. Phthalonitrile-based high temperature resin. *J. Polym. Sci. Part A: Polym. Chem.* **1988**, *26*, 3199–3212.
25 Keller, T. M. Synthesis and polymerization of multiple aromatic ether phthalonitriles. *Chem. Mater.* **1994**, *6*, 302–305.
26 Timoshkin, I. A.; Aleshkevich, V. V.; Afanas'eva, E. S.; Bulgakov, B. A.; Babkin, A. V.; Kepman, A. V.; Avdeev, V. V. Heat-resistant carbon fiber reinforced plastics based on a copolymer of bisphthalonitriles and bisbenzonitrile. *Polym. Sci. Ser. C* **2020**, *62*, 172–182.
27 Wang, G.; Han, Y.; Guo, Y.; Sun, J.; Wang, S.; Zhou, H.; Zhao, T. Phthalonitrile terminated fluorene based copolymer with outstanding thermal and mechanical properties. *Eur. Polym. J.* **2019**, *113*, 1–11.
28 Ye, J.; Li, Q.; Zhang, S.; Liu, X. Melamine modified phthalonitrile resins: Synthesis, polymerization and properties. *Polymer* **2022**, *256*, 125156.
29 Chen, M.; He, X.; Lv, J.; Tan, W.; Wang, Y.; Hu, J.; Zeng, K.; Yang, G. A new bio-based thermosetting with amorphous state, sub-zero softening point and high curing efficiency. *Polymer* **2023**, *264*, 125518.
30 Ma, A.; Rong, J.; Li, D.; Chen, X.; Yu, X.; Zhang, Q. Thermal stability and curing mechanism of self-catalytic bio-based phthalonitrile resins. *Polymer* **2025**, *336*, 128916.
31 Xu, F.; Sha, Z.; Zhuo, L.; Chang, W.; Sun, B.; Wang, C. H.; Gu, B.; Zhang, J. Improving thermal stability and mechanical properties of high temperature carbon fibre phthalonitrile resin composites *via* nano-CuO modified matrices. *Compos. Part A Appl. Sci. Manuf.* **2025**, *197*, 109035.
32 Li, Q.; Zhang, S.; Ye, J.; Liu, X. Multiple catalytic polymerization of phthalonitrile resin bearing benzoxazine moiety: greatly reduced curing temperature. *Eur. Polym. J.* **2022**, *180*, 111472.
33 Lv, J.; Hong, J.; Liang, B.; Zhao, E.; Zeng, K.; Chen, M.; Hu, J.; Yang, G. Study of the curing kinetics of melamine/phthalonitrile resin system. *Thermochim. Acta* **2020**, *683*, 178442.
34 Gao, C.; Gu, H.; Du, A.; Zhou, H.; Pan, D.; Naik, N.; Guo, Z. Polyaniline facilitated curing of phthalonitrile resin with enhanced processibility and mechanical property. *Polymer* **2021**, *219*, 123533.
35 Sastri, S. B.; Keller, T. M. Phthalonitrile cure reaction with aromatic diamines. *J. Polym. Sci. Part A Polym. Chem.* **1998**, *36*, 1885–1890.
36 Badshah, A.; Kessler, M. R.; Heng, Z.; Hasan, A. Synthesis and characterization of phthalonitrile resins from ortho-linked aromatic and heterocyclic monomers. *Polym. Int.* **2014**, *63*, 465–469.

37 Laskoski, M.; Neal, A.; Schear, M. B.; Keller, T. M.; Ricks-Laskoski, H. L.; Saab, A. P. Oligomeric aliphatic–aromatic ether containing phthalonitrile resins. *J. Polym. Sci. Part A Polym. Chem.* **2015**, *53*, 2186–2191.

38 Zeng, K.; Hong, H.; Zhou, S.; Wu, D.; Miao, P.; Huang, Z.; Yang, G. A new soluble aramide with pendant phthalonitrile units and polymer property enhancement by nitrile cure reactions. *Polymer* **2009**, *50*, 5002–5006.

39 Kirmani, M. H.; Ramachandran, J.; Arias-Monje, P. J.; Gulgunje, P.; Kumar, S. The effects of processing and carbon nanotube type on the impact strength of aerospace-grade bismaleimide based nanocomposites. *Polym. Eng. Sci.* **2022**, *62*, 1187–1196.

40 Lan, K.; Deng, Y.; Huang, A.; Li, S. Q.; Liu, G.; Xie, H. L. Highly-performance polyimide as an efficient photothermal material for solar-driven water evaporation. *Polymer* **2022**, *256*, 125177.

41 Jiao, Y.; Yuan, L.; Liang, G.; Gu, A. Dispersing carbon nanotubes in the unfavorable phase of an immiscible reverse-phase blend with Haake instrument to fabricate high-k nanocomposites with extremely low dielectric loss and percolation threshold. *Chem. Eng. J.* **2016**, *285*, 650–659.

42 Lyu, J.; Ji, B.; Wu, N.; Liao, W.; Yin, C.; Bai, S.; Xing, S. The effect of substituent group in allyl benzoxazine on the thermal, mechanical and dielectric properties of modified bismaleimide. *React. Funct. Polym.* **2023**, *191*, 105673.

43 Xie, H.; Chen, S.; Qu, B.; Liu, X.; Li, W.; Wang, R.; Hou, L.; Zhuo, D. Preparation of silicone-bismaleimide photosensitive resin and its application in 3D printing. *J. Sci. Adv. Mater. Devices* **2026**, *11*, 101099.

44 Jiang, M.; Xu, M.; Jia, K.; Liu, X. Copolymerization of self-catalyzed phthalonitrile with bismaleimide toward high-temperature-resistant polymers with improved processability. *High Perform. Polym.* **2016**, *28*, 895–907.

45 Zhang, B.; Liu, F.; Chen, S.; Huang, L.; Zhong, Y.; Fan, W.; Li, J. Fluorine bismaleimide resin with outstanding piezoelectric characteristics for structure-function integrated composites. *Chem. Eng. J.* **2025**, *503*, 158506.

46 Zhu, X.; Yin, S.; Liu, L.; Yi, W.; Luo, G.; Zhao, Z.; Chen, W. Effects of temperature on mechanical properties and impact resistance of carbon fiber/bismaleimide resin composites. *J. Mater. Res. Technol.* **2025**, *34*, 2553–2569.

47 Kaliavaradhan, K.; Muthusamy, S. Synthesis and characterization of various phenylene diamine-based bismaleimide-containing phthalonitrile resins. *Polym. Bull.* **2016**, *73*, 1921–1938.

48 Nechausov, S. S.; Aleksanova, A. A.; Morozov, O. S.; Bulgakov, B. A.; Babkin, A. V.; Kepman, A. V. Low-melting phthalonitrile monomers containing maleimide group: synthesis, dual-curing behavior, thermal and mechanical properties. *React. Funct. Polym.* **2021**, *164*, 104932.

49 ASTM: D2344/D2344M-00e1. Standard test method for short-beam strength of polymer matrix composite materials and their laminates.

50 Liu, Z.; Liu, Y.; Peng, W.; Lu, Z.; Liang, B.; Liu, Y.; Li, C.; Hu, J.; Zeng, K.; Yang, G. New model phthalonitrile resin system based on self-promoted curing reaction for exploring the mechanism of radical promoted-polymerization effect. *J. Appl. Polym. Sci.* ***2019***, *136*, 48134.

51 Torrecillas, R.; Regnier, N.; Mortaigne, B. Thermal degradation of bismaleimide and bisnadimide networks—products of thermal degradation and type of crosslinking points. *Polym. Degrad. Stab.* **1996**, *51*, 307–318.

52 Liu, C.; Li, S.; Yuan, Z.; Xue, S.; Sun, M.; Zhang, X.; Li, J.; Xue, G.; Bai, X.; Liu, W.; Zhang, B. Low-melting maleimide-containing phthalonitrile resins: synthesis, curing behavior, and thermal performance. *Polymer* **2024**, *315*, 127821.

53 Xu, M.; Ren, D.; Chen, L.; Li, K.; Liu, X. Understanding of the polymerization mechanism of the phthalonitrile-based resins containing benzoxazine and their thermal stability. *Polymer* **2018**, *143*, 28–39.

54 Wang, G.; Guo, Y.; Han, Y.; Li, Z.; Ding, J.; Jiang, H.; Zhou, H.; Zhao, T. Enhanced properties of phthalonitrile resins reinforced by novel phthalonitrile-terminated polyaryl ether nitrile containing fluorene group. *High Perform. Polym.* **2020**, *32*, 3–11.

55 Wu, Z.; Wang, S.; Zong, L.; Li, N.; Wang, J.; Jian, X. Novel phthalonitrile-based composites with excellent processing, thermal, and mechanical properties. *High Perform. Polym.* **2018**, *30*, 720–730.

56 Hu, J.; Hu, Y.; Deng, S. F.; Zhou, J. L.; Jiang, N.; Zhu, Y.; Sun, M. Synthesis and properties of a novel silicon-containing phthalonitrile resin and its quartz-fiber-reinforced composites. *High Perform. Polym.* **2020**, *32*, 1112–1121.

57 Poliakova, D. I.; Morozov, O. S.; Nechausov, S. S.; Afanaseva, E. A.; Bulgakov, B. A.; Babkin, A. V.; Kepman, A. V.; Avdeev, V. V. Fast curing phthalonitrile modified novolac resin: synthesis, curing study and preparation of carbon and glass fiber composites. *React. Funct. Polym.* **2022**, *181*, 105450.

58 Mirbagheri, S. M. J.; Fattahi, H.; Mortezaei, M.; Ahmadi, M. The effect of amine and phenolic curing agents on curing temperature of high temperature phthalonitrile resin for preparation of high performance carbon/phthalonitrile composite. *J. Sci. Technol. Compos*. **2025**, *11*, 2569–2579 (in Persian).